

Controlled time series generation for automotive software-in-the-loop testing using GANs

Dhasarathy Parthasarathy^{†*}, Karl Bäckström^{*}, Jens Henriksson^{*§}, Sólrún Einarsdóttir^{*}

[†]Volvo Group, Gothenburg, Sweden, Email: dhasarathy.parthasarathy@volvo.com

^{*}Chalmers University of Technology, Gothenburg, Sweden, Email: {bakarl, slrn}@chalmers.se

[§]Semcon AB, Gothenburg, Sweden, Email: jens.henriksson@semcon.com

Abstract—Testing automotive mechatronic systems partly uses the software-in-the-loop approach, where systematically covering inputs of the system-under-test remains a major challenge. In current practice, there are two major techniques of input stimulation. One approach is to craft input sequences which eases control and feedback of the test process but falls short of exposing the system to realistic scenarios. The other is to replay sequences recorded from field operations which accounts for reality but requires collecting a well-labeled dataset of sufficient capacity for widespread use, which is expensive. This work applies the well-known unsupervised learning framework of Generative Adversarial Networks (GAN) to learn an unlabeled dataset of recorded in-vehicle signals and uses it for generation of synthetic input stimuli. Additionally, a metric-based linear interpolation algorithm is demonstrated, which guarantees that generated stimuli follow a customizable similarity relationship with specified references. This combination of techniques enables controlled generation of a rich range of meaningful and realistic input patterns, improving virtual test coverage and reducing the need for expensive field tests.

Index Terms—software-in-the-loop, generative adversarial networks, time series generation, latent space arithmetic

I. INTRODUCTION

Software-in-the-loop (SIL) is a commonly used technique for developing and testing automotive application software. In a typical SIL setup, the System Under Test (SUT) is a combination of the application software and software representations of related physical and virtual entities. By executing the mechatronic SUT in a purely virtual environment, SIL testing enables continuous integration and verification with faster test feedback [1]. The extent and fidelity of virtual execution are usually defined by the test objective. This work focuses on one important component of the system environment – input stimuli. Input stimulation in a SIL setup can be challenging since ranges are often large and continuous, with developers/testers aiming for systematic coverage, while trading off concerns such as cost and duration of testing, coherence of test results, and confidence in covering corner cases.

A. Challenges in current practice

One technique for sampling the input space is to craft templates, designed to capture characteristics that are interesting for the test. The Worldwide harmonized Light-duty vehicles Test Cycles (WLTC) [2], for example, are designed to represent driving cycles (time series of vehicle and/or

engine speed) under typical driving conditions, and are popular for benchmarking drive train applications. Standard templates apart, it is common practice for a tester to craft custom templates for a test case. Templates, as seen in Fig 1a of a vehicle starting and stopping, enable testers to perform controllable and repeatable tests. When templates need to be more realistic, testers spend significant effort in finding the right function approximations. Templates, no matter how complex, bear the risk of not covering realistic scenarios experienced in the field.

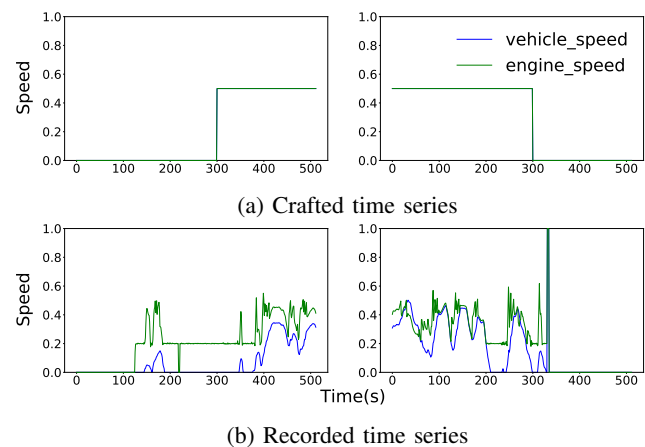


Fig. 1: Two approaches of input stimulation (speed values rescaled to [0,1])

To better approximate reality, a common practice in the automotive industry is to apply real-world input stimuli that are recorded from vehicles in the field. Examples can be seen in Fig 1b, which show recorded sequences of a vehicle starting and stopping. To control the test process, testers need to identify those exact sequences which possess desired characteristics. A special case, fault tracing, occurs when a tester chooses sequences during which faults are known (or suspected) to have occurred. To test using the right field-recorded sequences, one needs a manageable data set of labeled sequences to choose from, which is an expensive requirement. Additionally, literal signal replay, while helpful in recreating field scenarios, has the limitation of being largely restricted to what is recorded. In practice, finding the right balance between the two techniques of input stimulation is a perennial concern. This limits applicability and the overall confidence in SIL testing.

B. Contributions

While drawbacks do exist in each approach, it is easy to see that both real-world and designed stimuli have good utility. Bridging between the two approaches, this work demonstrates a method for controlled generation of realistic synthetic stimuli. Specifically, we contribute:

- A Variational Autoencoder-Generative Adversarial Network (VAE/GAN) model for producing synthetic vehicle signal sequences for SIL testing
- A method to generate realistic SIL stimuli that are measurably similar to reference stimuli, improving chances of discovering bugs
- A method to customize stimulus generation using similarity metrics

Together, these techniques give better control in covering the input space and ease the test process.

C. Scope

While the focus is on controlled generation of time series of in-vehicle signals (information exchanged between on-board applications), our results may be applicable to time series generation in other domains. With signals being both discrete and continuous-valued, the scope of this work is limited to the latter, since covering continuous input ranges is a pressing challenge in SIL testing.

D. Structure

Forthcoming sections present a survey of related techniques (Section II), followed by an introduction of the data and model architecture (Section III). Then comes the presentation on using similarity metrics in model training and evaluation (Section IV), and in controlled generation of synthetic stimuli (Section V). This is followed by a discussion on the idea of similarity with references as a plausibility measure (Section VI), and the conclusion (Section VII).

II. RELATED WORK

Following its introduction [3], GANs have been applied for synthetic data generation in a variety of domains. Reflecting our scope, we focus on surveying reports of continuous-valued sequence generation and highlighting the following aspects – (i) the model architecture and (ii) measures to check plausibility of generated samples.

Using a recurrent GAN, generation of real-valued medical time-series was demonstrated by [4], where two plausibility measures were shown. One is measuring Maximum Mean Discrepancy (MMD) [5] between populations of real and synthetic samples, and the other to train a separate model using synthetic/real data and evaluate it using real/synthetic data. Using a recurrent architecture, [6] demonstrated music generation, with generated samples evaluated using observable features such as polyphony and repetitions. From an application perspective, [7] comes close, where a recurrent GAN was applied to generate time series of automotive perception sensors, for simulation-based verification. Plausibility is shown using the Jensen-Shannon (JS) divergence, as a

measure of symmetric relative entropy between populations of real and generated samples. A combined Long-Short Term Memory (LSTM) and Mixture Density Network (MDN) GAN for generating sensor data has been shown by [8], where GAN loss and discriminator prediction are used as evaluation measures. Convolutional GANs have been applied for sequence generation in [9] and [10]. Both of them apply MMD and Wasserstein-1 [11], while the latter additionally applies classical machine learning methods like k-means clustering to measure plausibility. Beyond deep generative models, purely statistical methods of generating and evaluating time series (examples [12] and [13]) have been reported. However, such methods are, in the existing literature, inherently dependent on features selected by a domain expert. In comparison, a *deep learning* or *GAN* approach provides the capability to learn the necessary features automatically, thus being able to optimally adapt to the dataset on which it is applied.

The SIL testing process normally involves test case design, where the right (class of) input stimuli, *the reference*, are chosen or constructed to meet the test objective. Therefore, unlike most reported applications, to maximize confidence, SIL stimulus generation must verifiably comply with the reference. We show how such compliance can be guaranteed using a novel combination of network architecture and metric-based search.

III. MODEL SETUP

The following sections describe the chosen model architecture and dataset. All code and data used in this work is publicly available¹.

A. Choosing the VAE/GAN architecture

Generative models learn to encode information about a distribution of samples x in the form of a concise representation. The GAN uses a *representation* \rightarrow *generator* \rightarrow *discriminator* architecture. Given the latent representation $z \sim p(z)$, a generator network maps it to a data sample $\bar{x} \sim Gen(z)$, whose membership in the sample distribution is assessed by the discriminator network $Disc(\bar{x})$. Training the GAN involves playing the minimax game, minimizing the objective in Eq 1 [3]. The generator tries to fool the discriminator with synthetic samples, while the discriminator criticizes generated samples.

$$\mathcal{L}_{GAN}^* = \log(Disc(x)) + \log(1 - Disc(Gen(z))) \quad (1)$$

The alternative Variational Autoencoder (VAE) uses the *encoder* \rightarrow *representation* \rightarrow *decoder* architecture. Given a sample x , it uses an encoder network to map it to a latent representation $z \sim q(z|x) = Enc(x)$ and a decoder network to reconstruct an estimate of the original sample $\bar{x} \sim p(x|z) = Dec(z)$. Training the VAE involves minimizing element-wise reconstruction error between x and \bar{x} (Eq 2), while jointly using a regularization term (Eq 3) [14] that encourages smoother encoding of the latent space.

¹<https://github.com/dhas/LoGAN.git>

$$\mathcal{L}_{elem} = -\mathbb{E}_{q(z|x)}[\log \bar{x}] \quad (2)$$

$$\mathcal{L}_{prior} = -\mathbb{E}_{q(z|x)}[\log(p(x|z))] \quad (3)$$

In any case, synthetic samples are generated by sampling z and mapping it to \bar{x} . As noted earlier, in many SIL scenarios, testers are interested in stimuli that are similar to a reference, whether designed or field-recorded. Having a reference stimulus available as the starting point, an architecture with an encoder readily locates it in the latent space, easing the sampling process. While VAE seems suitable, it has well-recognized drawbacks in using element-wise reconstruction loss, which results in generated samples of poorer quality compared to those generated by a GAN. One alternative is the VAE/GAN model, which combines both frameworks and has an *encoder* \rightarrow *representation* \rightarrow *generator* \rightarrow *discriminator* architecture (Fig 2). Since the discriminator learns the essential features of a convincing sample, a better measure of reconstruction would be the distance between real and generated samples at the l^{th} -layer of the discriminator (Eq 4). By minimizing \mathcal{L}_{Disl} instead of element-wise reconstruction, and by additionally discriminating reconstructed samples (Eq 5), the VAE/GAN has been shown [15] to generate samples of better quality than VAE. With the double advantage of being able to encode the reference and generate samples of good quality, VAE/GAN is a good starting point for SIL stimulus generation.

$$\mathcal{L}_{Disl} = -\mathbb{E}_{q(z|x)}[\log p(Disc_l(x)|z)] \quad (4)$$

$$\mathcal{L}_{GAN} = \mathcal{L}_{GAN}^* + \log(1 - Disc(Dec(Enc(x)))) \quad (5)$$

$$\mathcal{L} = \beta \mathcal{L}_{prior} + \gamma \mathcal{L}_{Disl} + \mathcal{L}_{GAN} \quad (6)$$

B. The data set

To illustrate our technique of controlled generation, fixed-length time series of two signals of interest, *vehicle and engine speed*, were chosen. While any other set of signals can conceivably be chosen, the chosen set of two is a good starting point since they influence a broad range of on-board applications. The primary source of data is a set of signals, recorded in a fleet of 19 Volvo buses over a 3–5 year period. From this source, 100k 512-sample long unlabeled sequences of the signals of interest were collected to form the training set. Fixing the length and aligning the sequences helps treating them like images, allowing easy use of standard convolutional GAN architectures. An additional test set of 10k samples was collected. In this test set, a sparse labeling activity was conducted to pick sequences with desired characteristics. Examples of identified start and stop sequences were already seen in Fig 1b. More samples from the test set can be seen in Fig 10 in the appendix.

C. Designing the model

Having fixed the sequence length, upon trial-and-error in architecture selection, the encoder, decoder/generator, and discriminator are designed as 4-layer 1D convolutional neural networks. The kernel and mini-batch sizes, both influential

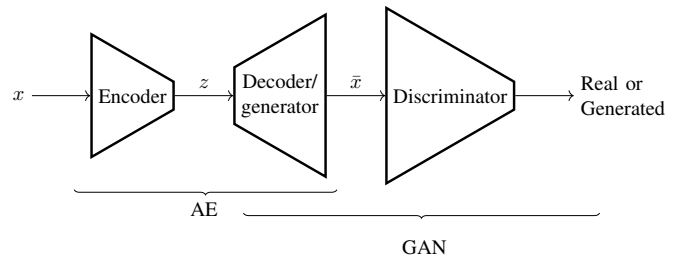


Fig. 2: The VAE/GAN model

hyper-parameters, are fixed to 8 and 128 respectively. Closely following the original VAE/GAN objective, the composite network is trained by minimizing the triple criteria set by Eq 6. Two additional hyperparameters are introduced, β following the β -VAE model, which encourages disentanglement [16] between latent variables, and γ , which, as suggested in [15], allows weighing the influence of reconstruction against discrimination. Among suggestions in [17] to improve stability of GAN training, using the Adam optimizer with a learning rate of $2 \cdot 10^{-4}$ and a momentum of 0.5 greatly helped in achieving training convergence, while the recommendation of using *LeakyReLU* and *tanh* activations did not. Based on visual inspection, *ReLU* and *sigmoid* activations are found to produce samples of better quality, perhaps because of a significant amount of baseline-zero values in recorded signals, when the buses were turned off.

IV. METRIC GUIDED TRAINING AND EVALUATION

GAN training is widely acknowledged as challenging, with *Gen* and *Disc* loss trends being the standard indicator of training progress. Tracking objectives during training does provide valuable feedback on model design and parameter selection. However, when it comes to assessing the quality of generated data, they are indirect at best. Testers, who are mainly interested in assessing the quality of generated stimuli, are better advised by direct measures. While visual inspection is common in the image domain, a quantitative alternative is the inception score [18], where generated images are evaluated by the widely-benchmarked Inception v3 model. In the absence of such a benchmark for in-vehicle signal time series, or perhaps even time series in general, alternative metrics are necessary.

A. Choosing metrics for evaluation

As described earlier, setting up a SIL test involves choosing right stimulus patterns. Having picked a reference pattern, testers normally vary it in some predictable fashion, with variations expected to be structurally related to the reference. Combinatorially designing these variations, which is common standard practice, may make it easy to enforce the structural relationship, but can be overwhelming as sequences grow longer. Generated stimuli do eliminate the need for such manual design, but they remain useful only as long as they show a structural relationship with the reference. To enforce this, one can turn to a number of similarity measures, some of which were mentioned in Section II. However, with references

simply being a handful of sequences (the fewer the easier for test design), metrics that specialize in measuring pair-wise similarity are more intuitive. Specifically, we consider:

- Dynamic Time Warping (DTW) [19] – which is an objective measure of similarity between two sequences. DTW is a measure of distance and therefore a non-negative real number. Lower values indicate higher similarity.
- Structural Similarity Index (SSIM) [20] – which is an objective measure of similarity between two images. SSIM between a pair of images is a real number between 0 (dissimilar) to 1 (similar)

With our sequences being time series, DTW is perhaps a natural fit. SSIM may consider its input signals to be images, but it does not exclude itself from comparing aligned sequences of fixed length. It also has the advantage of being a number in the range (0, 1), making it easy to inspect. More important to note is that testers need to choose the right metric that helps meet the test objective.

B. Calibrating metrics during training

Having introduced objective similarity metrics, a calibration exercise helps in understanding their overall relationship with the model. It also gives the advantage of observing training progress through measures that are more intuitive than the training objective. A natural first step is to relate objective metrics with their subjective counterpart, the VAE/GAN similarity metric. Denoting reconstruction of sample(s) x as $\bar{x} = Dec(Enc(x))$, one notes that \mathcal{L}_{Disl} is calculated between x and \bar{x} on each training batch, as a measure of sample reconstruction in the training objective. Extending this idea, upon measuring the similarity between x and \bar{x} on a separate test batch, using \mathcal{L}_{Disl} , DTW and SSIM, one arrives at a

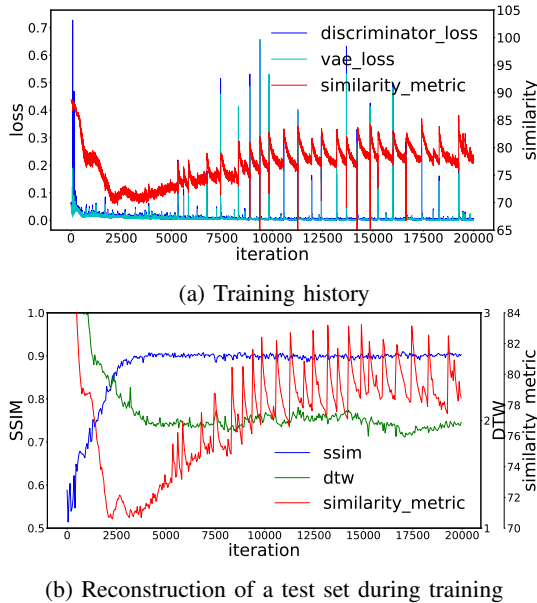


Fig. 3: Successfully training a model with β -250, γ -100 and 10 latent dimensions, using the Adam optimizer [21]

calibrated, generalized, and objective measure of the model’s reconstruction fitness.

As prescribed in [15], each training iteration consists of performing mini-batch gradient descent sequentially on the encoder ($\mathcal{L}_{Disl} + \beta\mathcal{L}_{prior}$), the decoder ($\gamma\mathcal{L}_{Disl} - \mathcal{L}_{GAN}$), and the discriminator (\mathcal{L}_{GAN}), averaged over 5 mini-batches. An example of a successful training regime can be seen in Fig 3. Convergence trends can be clearly spotted for the VAE/GAN similarity metric (Fig 3a), which converges around 10k iterations. In fact, there is no observable gain in average test set reconstruction SSIM (Fig 3b) beyond ~ 0.9 after 3k iterations. DTW seems to take a longer time to settle at ~ 2 , pointing to higher sensitivity than SSIM. The ‘lag’ between metrics in showing convergence is understandable, given their individual capabilities. However, the combined picture they present increases confidence in training convergence.

In contrast, an unsuccessful training regime is shown in Fig 4. Training objectives (Fig 4a) present a mixed picture, with the VAE/GAN similarity metric on a slow downward trend without the oscillations found in the successful case. Loss function trends are largely similar to those in the success case. The collapse in SSIM to ~ 0.6 and DTW to ~ 4 (Fig 4b), however, makes it clear that there is indeed no convergence in training. While such a clean indication is not always available, measuring reconstruction fitness using objective metrics does seem to give more intuitive feedback on the training process than the raw training objective. It is also clear that a major challenge lies in developing the notion of a good similarity score, requiring careful metric calibration on the dataset. In our case, we visually inspected the reconstruction of 15 randomly drawn samples from the test set to develop a notion that SSIM > 0.9 is healthy (for example, Fig 6c and Fig 6d).

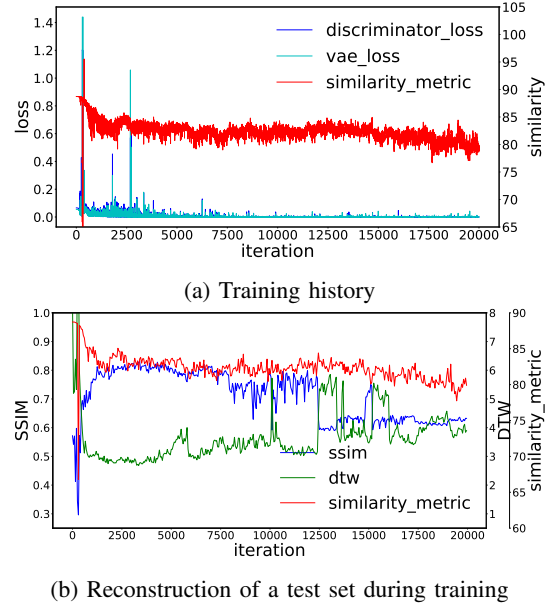


Fig. 4: Unsuccessfully training a model with β -250, γ -100 and 10 latent dimensions, using the RMSProp optimizer [21]

C. Using metrics to evaluate generator models

Consider, for example, the task of evaluating models in Table I. As seen in Fig 5, SSIM and DTW show quantitative differences between models' reconstruction fitness. The model e_5 , with highest average reconstruction SSIM and lowest average reconstruction DTW, best reconstructs the test set. While increasing the number of latent dimensions from 5 to 10 seems to increase reconstruction quality, more model samples are necessary to draw conclusions on the influence of β . We have thus shown a metric driven technique, of reasonable cost, that provides direct and intuitive feedback on generator quality both during and after training.

TABLE I: Explored model configurations, $\gamma=100$ in all cases

Name	Latent dims	β
e_1	5	1
e_2	5	10
e_3	5	50
e_4	5	250
e_5	10	1
e_6	10	10
e_7	10	50
e_8	10	250

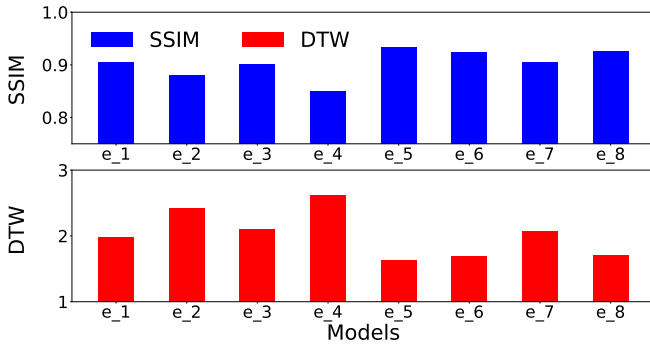


Fig. 5: Average (top) SSIM and (bottom) DTW between the test set and its reconstruction, for models in Table I

V. METRIC GUIDED STIMULUS GENERATION

The notion of similarity measurement is now extended to the original objective of helping testers generate stimuli in a controllable fashion.

A. Metric guided interpolation

Consider the case of testing SUT behavior when the vehicle comes to a halt. The tester could come up with a template x_1 (Fig 6a) as a reference. The template, while capturing the basic idea of the vehicle stopping, is not very realistic. To compensate, the tester could turn to another reference – a recorded signal showing a similar characteristic (Fig 6c). Generating plausible intermediate sequences between references x_1 and x_2 , with controlled introduction of elements of reality, is a well-structured, realistic, test of stopping behavior.

In any GAN model, the latent space z encodes a representation of the data distribution. Given x_1 and x_2 , it has been demonstrated (most notably in [17]) that linear

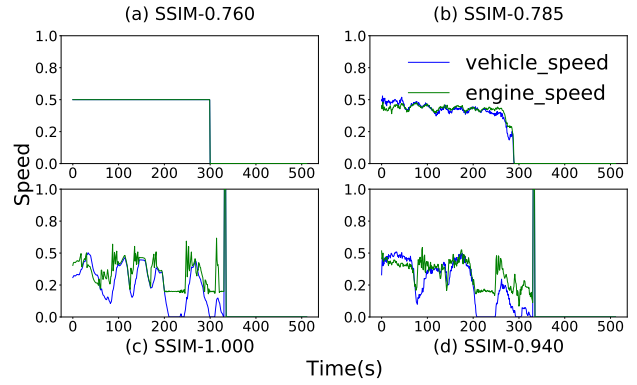


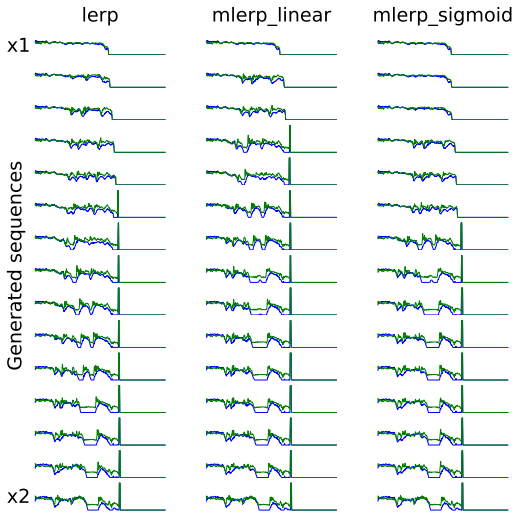
Fig. 6: (a) Interpolation source x_1 (b) and its reconstruction, (c) interpolation target x_2 , and (d) its reconstruction. All SSIM values are measured against x_2 . Speed values rescaled to $[0,1]$

interpolation between $z_1 = Enc(x_1)$ and $z_2 = Enc(x_2)$, yields points z_l , which, upon decoding $\bar{x}_l = Dec(z_l) \forall l$, represents a smooth transition between x_1 and x_2 in x space. Let us now examine this for the case of constructing intermediate sequences between chosen references x_1 and x_2 . One immediately noticeable advantage is that even a simplistic stop template is rendered, upon reconstruction, into a much more plausible form (Fig 6 a and c). The model is therefore a powerful alternative to classical function approximations. While a set of intermediate samples can be readily generated by naive linear interpolation, its plausibility as valid stimuli is vastly enhanced if generated samples show a smooth change in SSIM. Noting that *Decoder* and *SSIM* are continuous in their respective domains, it follows from the intermediate value theorem that an iterative search along the straight line between z_1 and z_2 gives a set of points which, when decoded, represents an arbitrarily smooth increase in SSIM. The granularity of the search is decided by the sampling ratio s .

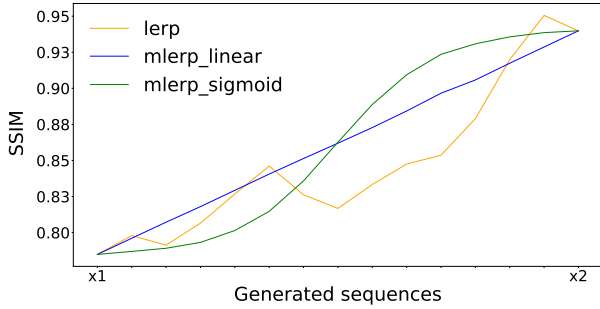
Algorithm 1: MLERP

Input : Start position z_0 , end position z^* , n.o. waypoints no_wps , model m , metric f_m , sampling ratio s
Output : Intermediate latent space positions z_s

- 1 $x^* \leftarrow m.generate(z^*)$
- 2 $start_metric \leftarrow f_m(m, z_0, x^*)$
- 3 $stop_metric \leftarrow f_m(m, z^*, x^*)$
- 4 $wps \leftarrow interp(start_metric, stop_metric, no_wps)$ # interpolation in metric space
- 5 $z_s \leftarrow linspace(z_0, z^*, no_wps)$ # initialize with linspace
- 6 $num_steps \leftarrow s \cdot |waypoints|$
- 7 **for** $i \in [num_steps]$ **do**
- 8 $pos \leftarrow z_0 + \frac{i}{num_steps}(z^* - z_0)$
- 9 $m_{pos} \leftarrow f_m(m, pos, z^*)$
- 10 $wp_ind \leftarrow argmin_{i \in [wps]} (|wps[i] - m_{pos}|)$ # find closest waypoint in metric space
- 11 $m_z \leftarrow f_m(m, z_s[wp_ind], z^*)$
- 12 **if** $m_{pos} < m_z$ **then**
- 13 $z_s[wp_ind] \leftarrow pos$
- 14 **end**
- 15 **end**



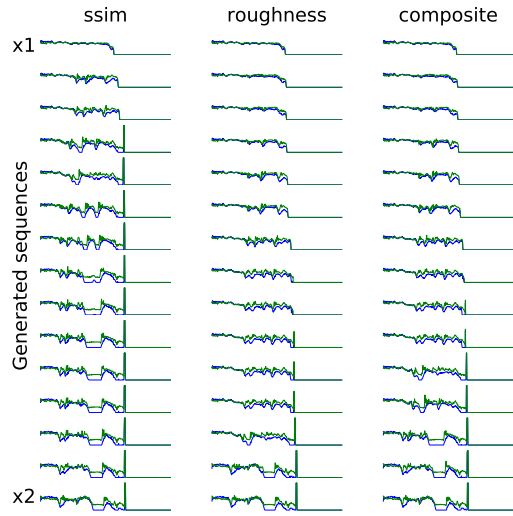
(a) Generated samples



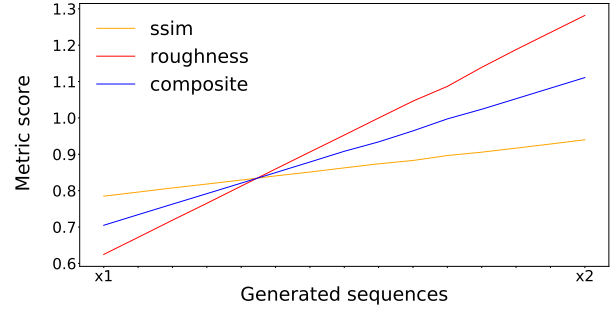
(b) SSIM of generated samples

Fig. 7: Generating intermediate samples between template (x_1) and real-world (x_2) stop sequences with e_5 using naive linear interpolation (*lerp*), MLERP with linear increase in SSIM $s=15$ (*mlerp_linear*), and MLERP with sigmoid increase in SSIM and $s=30$ (*mlerp_sigmoid*)

To achieve this, we propose the metric based linear interpolation algorithm MLERP (Algorithm 1) which interpolates in *metric* space, as opposed to the latent. Given some desired division of the metric space (Algorithm 1 – step 4), MLERP will sample points along the straight line between z_1 and z_2 , while keeping track of the latent positions which correspond best to the metric space division. The metric f_m , sampling ratio s , number of waypoints no_wps , and metric space division wps are all tunable parameters. MLERP can be applied for generating a set of intermediate sequences whose SSIM changes smoothly between x_1 and x_2 . Observing the generated sequences themselves (Fig 7a) gives an indication of controlled variation. This is best seen in the *metric_sigmoid* case, where the resemblance with x_2 grows gradually because the metric space division wps is set as the logistic sigmoid function. In comparison, *mlerp_linear* is a case where resemblance grows rapidly, since wps is set to be linear. Fig 7b clearly shows that naive linear interpolation results in irregular increase in SSIM. MLERP, on the other hand, always guarantees a controllably smooth increase in SSIM.



(a) Generated samples



(b) Metric scores of generated samples

Fig. 8: Generating intermediate samples between template (x_1) and real-world (x_2) stop sequences, with e_5 , using MLERP with SSIM $s=15$ (*ssim*), R $s=100$ (*roughness*), and M_{sr} $\kappa=0.5$, $s=100$ (*composite*)

To further illustrate finely controlled generation, consider the composite metric M_{sr} (Eq 7). Here SSIM is combined with R , which is a simple measure of roughness/smoothness of a given sequence b , relative to the reference sequence a , calculated as a ratio of average absolute change in sample values. The effect of R is best seen in the *roughness* column in Fig 8a, where the smoothness of generated sequences steadily reduces, when compared to the *ssim* column, where sequences, guided by SSIM, steadily increase resemblance. Sequences generated using composite metric M_{sr} , as seen in the *composite* column in Fig 8a, shows how a compromise can be struck between these two metrics. Metric variation is best seen in Fig 8b, where metric interpolation using M_{sr} strikes a balance between MLERP using SSIM and R individually, usually at the cost of a higher s .

Using such a set of metric guided synthetic stimuli during a test run not only ensures that test inputs are *verifiably realistic*, but also that *variations are controllable*. These are the twin objectives that testers aim for, but find it difficult to achieve in current practice. While this is certainly beneficial

compared to the original choices of crafted and real-world stimuli, realizing full potential of this technique, depends upon choosing the right metric, which is not always trivial. Compared to naive interpolation, metric-search incurs an additional cost in sampling, which is decided by the sampling ratio s . Such a cost can be offset when stimulus generation happens less frequently than test case execution and when it is, in the best case, a one-time activity.

$$M_{sr}(x_2, \bar{x}) = \kappa SSIM(x_2, \bar{x}) + (1 - \kappa)R(x_2, \bar{x}) \quad (7)$$

$$R(a, b) = \frac{\sum_{i=0}^{N-1} |b_{i+1} - b_i|}{\sum_{i=0}^{N-1} |a_{i+1} - a_i|} \quad (8)$$

B. Metric guided neighborhood search

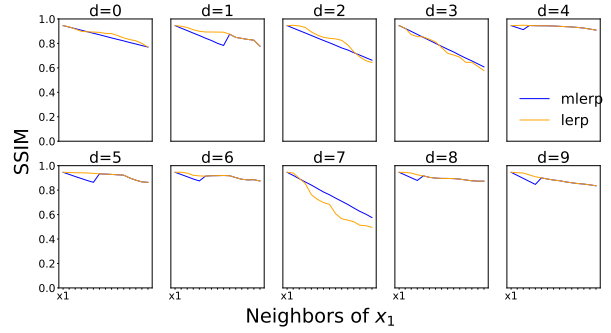
Given a stimulus sequence x_1 and its latent code z_1 , we know there exist samples of similar structure with latent codes in the neighborhood of z_1 . Metric driven sampling, solely along latent space axes, shows potential in identifying such neighbors, allowing testers to perform fine adjustments to x_1 . As seen in Fig 9a, with $\beta = 1$, MLERP between z_1 and $z_1[d]+ = 2$, along each latent space dimension d , is smoother than naive interpolation in 3 out of 10 cases. To keep search costs low, s is fixed to 30. Increased disentanglement ($\beta = 250$) shows larger and smoother change (Fig 9b) in SSIM, with same s , along more latent space dimensions. Examining variations in SSIM, along latent space axes, therefore helps in acquiring a quantitative notion of structure disentanglement. This can also be put to use, helping testers perform well informed adjustments in stimulus structure. By inspecting generated structural neighbors (Fig 11 in the appendix) and their SSIM with x_1 , testers can select the right adjustment that fits the test case. This expands the tester tool-kit by providing yet another method of stimulus design.

VI. SIMILARITY AS PLAUSIBILITY OF SYNTHETIC STIMULI

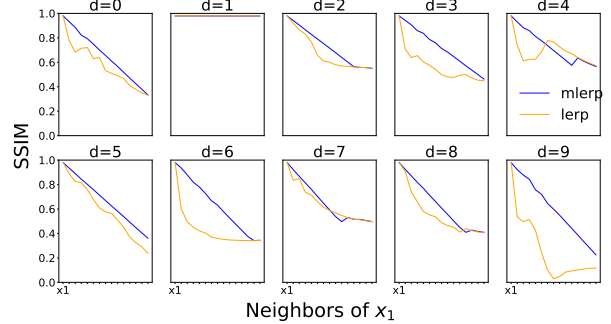
For generating time series stimuli, in automotive SIL testing, we have demonstrated the notion of *similarity with reference(s)* as a capable and quantitative measure of plausibility. Specifically, plausibility is ensured in three forms:

- Measuring reconstruction of a test set, similarity between x and $\bar{x} = Dec(Enc(x))$, as a fitness measure of the model
- Guided generation of intermediate sequences between x_1 and x_2 , by imposing a joint similarity relationship with x_1 and x_2 . Controllability is enhanced by crafting x_1 and choosing (a well corresponding) x_2 from recordings
- Guided generation of structural neighbors of a sequence x_1 , by imposing a similarity relationship with x_1

Assessing similarity using SSIM and DTW denote objective plausibility, but only in relation to a reference. While this technique obviously cannot judge the plausibility of a non-referenced, arbitrary set of generated samples, it bears no major consequence to SIL stimulus generation. Each test case has an objective to meet and, to control both execution and feedback, testers normally have a stimulus structure in mind, which can act as the reference. Identifying real-world



(a) Neighborhood search using e_5 ($\beta = 1$)



(b) Neighborhood search using e_8 ($\beta = 250$)

Fig. 9: Comparison of SSIM variations between neighborhood search using metric (mlerp) and naive (lerp) linear interpolation, along each latent space dimension d , between z_1 and $z_1[d]+ = 2$. Metric search was conducted with $s = 30$.

references, however, is a labeling activity, albeit sparse. For widespread practical use of this technique, the extent of sparse labeling that is needed remains to be seen.

VII. CONCLUSIONS

Integrating and testing automotive mechatronic systems is complex, where each mile of testing in the field increases time and cost to market. With a majority of feature growth in vehicles expected to come in the form of software, enhancing the capability of SIL verification is essential. As a step in this direction, we demonstrate a GAN-based framework to generate synthetic test stimuli. By exploiting the fact that testers often need to generate stimuli that follows a certain structure, we apply the VAE/GAN architecture and similarity metric-driven search for controlled generation of realistic synthetic stimuli. This achieves the twin objective of realistic but controllable stimulation, which helps expand the use of SIL testing. Future enhancements are certainly possible in network architecture to improve the quality of generated data and adaptation between templates and recordings. Easing metric design is important in making this technique practically easy to use and non-linear searching would also help reduce MLERP search costs. Additional work is necessary to close practical gaps in integration with a suitable SIL framework and deployment in a continuous integration pipeline. While such enhancements add value, the fundamental technique shows promise in broadening the applicability of SIL testing.

VIII. ACKNOWLEDGEMENTS

We thank Henrik Lönn and other colleagues at Volvo, Christian Berger, and Carl-Johan Seger for their helpful feedback.

This work was supported by the Wallenberg Artificial Intelligence, Autonomous Systems and Software Program (WASP), funded by the Knut and Alice Wallenberg Foundation.

REFERENCES

- [1] H. Kaijser, H. Lönn, P. Thorgren, J. Ekberg, M. Henningsson, and M. Larsson, "Towards Simulation-Based Verification for Continuous Integration and Delivery," in *ERTS 2018*, 9th European Congress on Embedded Real Time Software and Systems (ERTS 2018), (Toulouse, France), Jan. 2018.
- [2] U. Nations, "Addendum 15: Global technical regulation no. 15worldwide harmonized light vehicles test procedure," 2015.
- [3] I. J. Goodfellow, J. Pouget-Abadie, M. Mirza, B. Xu, D. Warde-Farley, S. Ozair, A. C. Courville, and Y. Bengio, "Generative adversarial nets," in *Advances in Neural Information Processing Systems 27: Annual Conference on Neural Information Processing Systems 2014, December 8-13 2014, Montreal, Quebec, Canada*, pp. 2672–2680, 2014.
- [4] C. Esteban, S. L. Hyland, and G. Rätsch, "Real-valued (medical) time series generation with recurrent conditional gans," *CoRR*, vol. abs/1706.02633, 2017.
- [5] B. K. Sriperumbudur, A. Gretton, K. Fukumizu, B. Schölkopf, and G. R. Lanckriet, "Hilbert space embeddings and metrics on probability measures," *J. Mach. Learn. Res.*, vol. 11, pp. 1517–1561, Aug. 2010.
- [6] O. Mogren, "C-RNN-GAN: continuous recurrent neural networks with adversarial training," *CoRR*, vol. abs/1611.09904, 2016.
- [7] N. M. Edvin Listo Zec, Henrik Arnelid, "Recurrent conditional gans for time series sensor modelling," in *Time Series Workshop at International Conference on Machine Learning*, (Long Beach, California), Jan. 2019.
- [8] M. Alzantot, S. Chakraborty, and M. B. Srivastava, "Sensegen: A deep learning architecture for synthetic sensor data generation," *CoRR*, vol. abs/1701.08886, 2017.
- [9] E. Brophy, Z. Wang, and T. E. Ward, "Quick and easy time series generation with established image-based gans," *CoRR*, vol. abs/1902.05624, 2019.
- [10] C. Zhang, S. R. Kuppannagari, R. Kannan, and V. K. Prasanna, "Generative adversarial network for synthetic time series data generation in smart grids," in *2018 IEEE International Conference on Communications, Control, and Computing Technologies for Smart Grids, SmartGridComm 2018, Aalborg, Denmark, October 29-31, 2018*, pp. 1–6, 2018.
- [11] S. Kolouri, S. R. Park, M. Thorpe, D. Slepcev, and G. K. Rohde, "Optimal mass transport: Signal processing and machine-learning applications," *IEEE Signal Processing Magazine*, vol. 34, pp. 43–59, July 2017.
- [12] Y. Kang, R. J. Hyndman, and F. Li, "GRATIS: generating time series with diverse and controllable characteristics," *CoRR*, vol. abs/1903.02787, 2019.
- [13] L. Kegel, M. Hahmann, and W. Lehner, "Feature-based comparison and generation of time series," in *Proceedings of the 30th International Conference on Scientific and Statistical Database Management, SSDBM 2018, Bozen-Bolzano, Italy, July 09-11, 2018*, pp. 20:1–20:12, 2018.
- [14] D. P. Kingma and M. Welling, "Auto-encoding variational bayes," in *2nd International Conference on Learning Representations, ICLR 2014, Banff, AB, Canada, April 14-16, 2014, Conference Track Proceedings*, 2014.
- [15] A. B. L. Larsen, S. K. Sønderby, H. Larochelle, and O. Winther, "Autoencoding beyond pixels using a learned similarity metric," in *Proceedings of the 33rd International Conference on Machine Learning, ICML 2016, New York City, NY, USA, June 19-24, 2016*, pp. 1558–1566, 2016.
- [16] I. Higgins, L. Matthey, A. Pal, C. Burgess, X. Glorot, M. Botvinick, S. Mohamed, and A. Lerchner, "beta-vae: Learning basic visual concepts with a constrained variational framework," in *5th International Conference on Learning Representations, ICLR 2017, Toulon, France, April 24-26, 2017, Conference Track Proceedings*, 2017.
- [17] A. Radford, L. Metz, and S. Chintala, "Unsupervised representation learning with deep convolutional generative adversarial networks," in *4th International Conference on Learning Representations, ICLR 2016, San Juan, Puerto Rico, May 2-4, 2016, Conference Track Proceedings*, 2016.

- [18] T. Salimans, I. Goodfellow, W. Zaremba, V. Cheung, A. Radford, X. Chen, and X. Chen, "Improved techniques for training gans," in *Advances in Neural Information Processing Systems 29* (D. D. Lee, M. Sugiyama, U. V. Luxburg, I. Guyon, I. Guyon, and R. Garnett, eds.), pp. 2234–2242, Curran Associates, Inc., 2016.
- [19] H. Sakoe and S. Chiba, "Dynamic programming algorithm optimization for spoken word recognition," *IEEE Transactions on Acoustics, Speech, and Signal Processing*, vol. 26, pp. 43–49, February 1978.
- [20] Zhou Wang, A. C. Bovik, H. R. Sheikh, and E. P. Simoncelli, "Image quality assessment: from error visibility to structural similarity," *IEEE Transactions on Image Processing*, vol. 13, pp. 600–612, April 2004.
- [21] S. Ruder, "An overview of gradient descent optimization algorithms," *CoRR*, vol. abs/1609.04747, 2016.

APPENDIX

A. Supporting figures

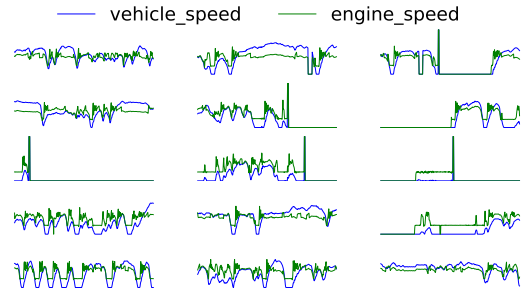


Fig. 10: Examples of recorded sequences from the test set (Speed values rescaled to [0,1])

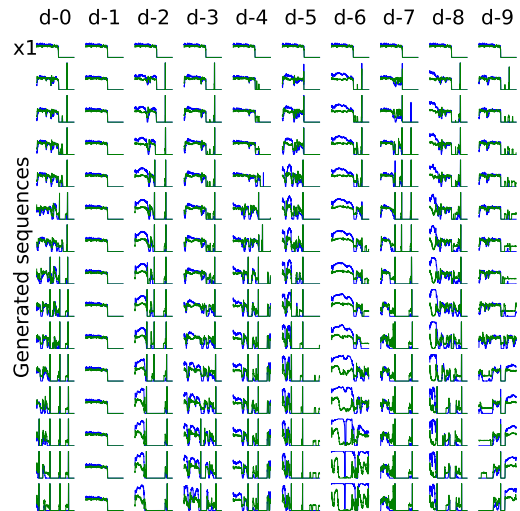


Fig. 11: Neighbors of the template stop sequence x_1 , generated with e_8 ($\beta = 250$), using metric-guided search. Each column represents interpolation along one latent space dimension d between z_1 and $z_1[d]^+ = 2$. Metric search was conducted with $s = 20$